

## CHAPTER

## 1

## Directory of Plates

Plate	Page	Topic	Objects	Wavelength domain/ $\lambda$	Grating
1	21	Overview of the spectral classes	1D-spectra of all basic spectral classes	3950–6690	200 L
2	22	Intensity profiles of all basic spectral classes		3950–6690	200 L
3	27	Spectral features of the late O class	Alnitak, $\zeta$ Ori Mintaka, $\delta$ Ori	3920–6710	200 L
4	28	Detailed spectrum of a late O-class star	Alnitak, $\zeta$ Ori	3950–4750 5740–6700	900 L
5	29	Spectral features of the early to middle O class, luminosity effect	$\theta^1$ Ori C 68 Cyg	3800–6700	200 L
6	33	Development of spectral features within the B class	Alnilam, $\epsilon$ Ori Gienah Corvi, $\gamma$ Crv	3900–6700	200 L
7	34	The effect of luminosity on spectra of the late B class	Regulus, $\alpha$ Leo Rigel, $\beta$ Ori $\varphi$ Sgr	3920–4750	900 L
8	35	Detailed spectrum of an early B-class star	Spica, $\alpha$ Vir	3800–6750 3900–4750 4800–5100 5700–6050 6450–6600	200 L 900 L 900 L 900 L 900 L
9	39	Development of spectral features within the A class	Castor, $\alpha$ Gem Altair, $\alpha$ Aql	3900–6800	200 L
10	40	Detailed spectrum of an early A-class star	Sirius A, $\alpha$ CMa	3900–6700 3900–4700 4780–5400	200 L 900 L 900 L
11	41	Effects of the luminosity on spectra of the early A class	Vega, $\alpha$ Lyr Ruchbah, $\delta$ Cas Deneb, $\alpha$ Cyg	3900–4700	900 L

*(cont.)*

Plate	Page	Topic	Objects	Wavelength domain/ $\lambda$	Grating
12	44	Development of spectral features within the F class	Adhafera, $\zeta$ Leo Procyon, $\alpha$ CMi	3830–6700	200 L
13	45	Effect of the luminosity on spectra of the early F class	Porrima, $\gamma$ Vir Caph, $\beta$ Cas Mirfak, $\alpha$ Per	3920–4750	900 L
14	49	Development of spectral features within the G class	Muphrid, $\eta$ Boo Vindematrix, $\epsilon$ Vir	3800–6600	200 L
15	50	Detailed spectrum of an early G-class star	Sun	3800–7200	200 L
	3900–4800			900 L	
16	51			4700–5700 5650–6700	900 L
17	52	Highly resolved Fraunhofer lines in the solar spectrum	Sun	5884–5899 5265–5274 5161–5186 4849–4871 4300–4345 3915–3983	SQUES echelle
18	57	Development of spectral features within the K class	Arcturus, $\alpha$ Boo Alterf, $\lambda$ Leo	3900–6800	200 L
19	58	Detailed spectrum of an early K-class star	Pollux, $\beta$ Gem	3900–6800 3800–4800	200 L 900 L
20	59	Detailed spectrum of a late K-class star	Aldebaran, $\alpha$ Tau	5150–5900 5850–6700	900 L
21	60	Luminosity effects on spectra of the late K class	Alsciaukat, $\alpha$ Lyn 61 Cyg B	4000–4900	900 L
22	64	Development of spectral features within the M class	Antares, $\alpha$ Sco Ras Algethi, $\alpha$ Her	3900–7200	200 L
23	65	Red dwarfs and flare stars	Gliese388 Gliese411	4200–7200	200 L
24	66	Effects of the luminosity on spectra of the late M class	Ras Algethi, $\alpha$ Her Gliese699	3900–7200	200 L
25	71	Mira variable M(e), comparison to a late-classified M star	Mira, o Cet Ras Algethi, $\alpha$ Her	3900–7200	200 L
26	75	Extreme S-class star, comparison to a Mira variable M(e)	R Cygni Mira, o Cet	4100–7300	200 L
27	76	Development of spectral features within the S class	Omicron1 Ori Chi Cyg R Cyg	4100–7300	200 L
28	77	Comparison of an “intrinsic” and “extrinsic” S-class star	BD Cam HR Peg	4300–7200	200 L
29	82	Comparison of differently classified carbon stars	WZ Cas Z Psc W Ori	4600–7300	200 L

(cont.)

Plate	Page	Topic	Objects	Wavelength domain/ $\lambda$	Grating
30	83	Merrill–Sanford bands, details at a higher resolved spectrum	W Ori	4730–5400	900 L
31	84	Carbon star with H $\alpha$ emission line	R Lep, Hind’s Crimson Star	5100–7300	200 L
32	88	White dwarfs with different spectral classifications	WD 0644 +375 40 Eri B Van Maanen’s Star	3900–6600	200 L
33	94	Wolf–Rayet stars, types WN and WC	WR133 WR140	3850–7250	200 L
34	95	Wolf–Rayet stars, types WN and WO	WR136 WR142	3860–7200 3750–7200	200 L
35	98	LBV star, early B class, P Cygni profiles	P Cyg, 34 Cyg	3900–6950 6000–6800	200 L 900 L
36	99	Detailed spectrum of LBV star, early B class, P Cygni profiles	P Cyg, 34 Cyg	3850–4650 4700–6050	900 L
37	103	Be star, early B class	Dschubba, $\delta$ Sco	3650–7000 4820–4940 6500–6700 6670–6690	200 L 900 L 900 L 900 L
38	104	Be star, early B class	Tsih, $\gamma$ Cas	3970–6750	200 L
39	107	Be shell star, comparison with an “ordinary” Be star	$\zeta$ Tau Dschubba, $\delta$ Sco	3800–6800	200 L
40	112	Herbig Ae/Be protostar	R Mon NGC 2261	3900–7200	200 L
41	113	Prototype of the T Tauri stars	T Tau	3900–7000	200 L
42	114	FU Orionis protostar, comparison with K0 giant	FU Ori Algieba, $\gamma$ Leo	3900–6800	200 L
43	120	Comparison of metallicity	Vega, $\alpha$ Lyr Sirius A, $\alpha$ CMa	3920–4700	900 L
44	121	Comparison of spectral classes Bp–Ap Hg–Mn and the reference profile of Vega	Alpheratz, $\alpha$ And Vega, $\alpha$ Lyr Cor Caroli, $\alpha^2$ CVn	4100–4220	SQUES echelle
45	122	Estimation flux density of mean magnetic field modulus	Babcock’s Star, HD 215441	small sections 4555–6380	SQUES echelle
46	129	Spectroscopic binaries: Detached SB2 systems	Spica, $\alpha$ Vir Mizar A, $\zeta$ UMa	6540–6580 6660–6690	SQUES echelle
47	130	Semi-detached system and eclipsing binary	Sheliak, $\beta$ Lyr	3800–7200	200 L
48	131	Semi-detached system and eclipsing binary, spectral details	Sheliak, $\beta$ Lyr	H $\alpha$ , H $\beta$ , He I 6678, 5876, 5016, 4921	SQUES echelle

*(cont.)*

Plate	Page	Topic	Objects	Wavelength domain/ $\lambda$	Grating
49	138	Classical nova: development of the spectrum during outburst	Nova V339 Del	4200–6800	Trans. 100 L
50	139	Recurrent nova in quiescence	T CrB	4100–7300	200 L
51	140	Dwarf nova	SS Cyg	3800–6800	200 L
52	141	Symbiotic star	EG And	3900–7200	200 L
53	148	Supernova type Ia, characteristic spectrum and chronology	SN2014 J Host galaxy M82	3800–7200	200 L
54	158	Absorption line galaxy: comparison with stellar G class	Andromeda M31 Vindemiatrix $\epsilon$ Vir	3900–6700	200 L
55	159	LINER galaxy	M94	3850–6900	200 L
56	160	Starburst galaxy	M82	4300–7000	200 L
57	161	Seyfert galaxy, AGN	M77	3800–6800	200 L
58	162	Quasar: emission lines	3C273	3800–6600	200 L
59	163	Quasar: redshift	3C273	4400–7600	200 L
60	164	Blazar, BL Lacertae object	Mrk 421	3950–7000	200 L
61	170	Stars of the open Pleiades cluster with emission line classification	17-, 23-, 25- and 28 Tau	3800–6700	200 L
62	171	Stars of the open Pleiades cluster with absorption lines	16-, 18-, 19-, 20-, 21- and 27 Tau	3800–6700	200 L
63	172	Integrated spectra of globular clusters	M3, M5, M13	3900–6700	200 L
64	185	Emission nebula: H II region	M42	3800–7300	200 L
65	186	Intensity profiles of H $\beta$ and [O III] ( $\lambda$ 5007) in the central area of M42	M42	n.a.	200 L
66	187	Post-AGB star with protoplanetary nebula	Red Rectangle HD 44179	3800–7000	200 L
67	188	Planetary nebula: excitation class E1	IC418 Spirograph Nebula	4100–7100	200 L
68	189	Planetary nebula: excitation class E3	NGC 6210 Turtle Nebula	3850–6600	200 L
69	190	Planetary nebula: excitation class E8	NGC 7009 Saturn Nebula	3800–6700	200 L
70	191	Planetary nebula: excitation class E10	M57 Ring Nebula	4600–6800	200 L
71	192	Intensity profiles of [O III] and [N II] in the longitudinal axis of M57	M57 Ring Nebula	n.a.	200 L
72	193	Estimation of the mean expansion velocity of a PN	NGC 7662 Blue Snowball Nebula	4950–5010	SQUES echelle
73	194	Emission nebula: SNR Excitation class E>5	Crab Nebula M1 NGC 1952	4600–6800	200 L

(cont.)

Plate	Page	Topic	Objects	Wavelength domain/ $\lambda$	Grating
74	195	Emission nebula: Wolf-Rayet Excitation Class E1	Crescent Nebula NGC 6888	4700–6800	200 L
75	196	Emission Nebula: Wolf-Rayet Star as its Ionizing Source Excitation Class E3	NGC 2359 Thor's Helmet, WR7, HD 56925	4000–7200 4500–6800	200 L 200 L
76	200	Reflectance Spectra of Mars and Venus	Mars, Venus	4300–7800	200 L
77	201	Reflectance Spectra of Jupiter and Saturn	Jupiter, Saturn	4400–7800	200 L
78	202	Reflectance Spectra of Uranus, Neptune and Titan	Uranus, Neptune, Titan	4500–7900	200 L
79	203	Spectra of Comet	C/2009 P1 Garradd	3800–6400	200 L
80	206	Telluric Absorptions in the Solar Spectrum	Earth's atmosphere	6800–7800	900 L
81	207	Telluric H <sub>2</sub> O Absorptions Around H $\alpha$ in the Spectra of the Sun and $\delta$ Sco	Sun $\delta$ Sco	6490–6610	SQUES echelle
82	208	Telluric Fraunhofer A and B Absorptions in Spectra of the Sun and $\delta$ Sco	Sun $\delta$ Sco	7590–7700 6865–6940	SQUES echelle
83	210	The Night Sky Spectrum	Light pollution airglow	4000–7400	200 L
84	217	Gas Discharge Lamp (Ne)	Neon glow lamp	5800–8100	900 L
85	218	Gas Discharge Lamp (ESL)	ESL Osram Sunlux	3900–6400	200 L
86	219	Gas Discharge Lamp (Na)	High pressure sodium vapor lamp	4700–7250	200 L
87	220	Gas Discharge Lamp (Xe)	Xenon high power lamp (Top of Mt. Rigi)	4900–6900	200 L
88	221	Calibration lamp with Ne, Xe	Modified glow starter Philips S10	3900–7200	200 L
89	222	Calibration Lamp with Ar	Modified glow starter OSRAM ST 111	3900–4800 4000–7700	900 L 200 L
90	223	Calibration Lamp with Ar, Ne, He Overview spectrum R~900	Modified glow starter RELCO 480	3800–7200	200 L
91	224	Calibration Lamp with Ar, Ne, He Highly Resolved Spectrum R~4000	Modified glow starter RELCO 480	3850–6300	900 L
92	225	Calibration Lamp with Ar, Ne, He Highly Resolved Spectrum R~4000	Modified glow starter RELCO 480	5900–8000	900 L
93	226	Calibration Lamp with Ar, Ne, He Highly Resolved Spectrum R~20,000	Modified glow starter RELCO 480	Order 28–32 6900–8160	SQUES echelle

*(cont.)*

Plate	Page	Topic	Objects	Wavelength domain/ $\lambda$	Grating
94	227	Calibration Lamp with Ar, Ne, He Highly Resolved Spectrum R~20,000	Modified glow starter RELCO 480	Order 33–37 5960–6930	SQUES echelle
95	228	Calibration lamp with Ar, Ne, He Highly resolved spectrum R~20,000	Modified glow starter RELCO 480	Order 38–42 5260–6000	SQUES echelle
96	229	Calibration lamp with Ar, Ne, He Highly resolved spectrum R~20,000	Modified glow starter RELCO 480	Order 43–47 4700–5300	SQUES echelle
97	230	Calibration lamp with Ar, Ne, He Highly resolved spectrum R~20,000	Modified glow starter RELCO 480	Order 48–52 4250–4770	SQUES echelle
98	231	Calibration lamp with Ar, Ne, He Highly resolved spectrum R~20,000	Modified glow starter RELCO 480	Order 53–57 3880–4315	SQUES echelle
99	232	Calibration lamp with Ar, Ne, He Image with SQUES echelle orders	Modified glow starter RELCO 480	Order 28–37 5970–8160	SQUES echelle
100	233	Calibration lamp with Ar, Ne, He Image with SQUES echelle orders	Modified glow starter RELCO 480	Order 38–47 4700–6020	SQUES echelle
101	234	Calibration lamp with Ar, Ne, He Image with SQUES echelle orders	Modified glow starter RELCO 480	Order 48–57 3750–4770	SQUES echelle
102	241	Swan bands/hydrocarbon gas flames: Comparison with a montage of spectra	Butane gas torch Comet Hyakutake WZ Cassiopeiae	3800–6400	200 L
103	242	Spectra of terrestrial lightning discharges	Integrated light of several lightning discharges	3750–7200	200 L

## CHAPTER

# 2 Selection, Processing and Presentation of the Spectra

## 2.1 Selection of Spectra

The main criteria for the selection of the spectra have been the documentation of the spectral characteristics and the demonstration of certain effects, for example due to the different luminosity classes. The consideration of bright “common knowledge stars” was of secondary importance. The ordinary spectral classes are presented here at least with an early and a rather late subtype to show the development of characteristic features in the profile. Further spectra are commented on in separate chapters such as extraordinary star types, emission nebulae, composite spectra of extragalactic objects, star clusters, reflectance spectra of solar system bodies, absorption bands generated by the Earth’s atmosphere and finally some profiles of terrestrial and calibration light sources.

## 2.2 Recording and Resolution of the Spectra

Except of a few clearly declared exceptions all spectra have been recorded by the author with the DADOS spectrograph, equipped with reflection gratings of 200 or 900 lines  $\text{mm}^{-1}$  [4]. Unless otherwise noted, the recording was made by an 8 inch Schmidt–Cassegrain Celestron C8, applying the 25  $\mu\text{m}$  slit of the DADOS spectrograph. Similar results could surely be achieved by applying other spectrographs, for example from Shelyak Instruments or other suppliers. To display some highly resolved spectral details, the SQUES echelle spectrograph was used, applying slit widths of 25–85  $\mu\text{m}$  [5]. Finally, most of the spectra have been recorded by the cooled monochrome camera ATIK 314L+, equipped with the Sony chip ICX285AL. A few spectra have been

recorded, in cooperation with Martin Huwiler, by the CEDES 36 inch telescope of the Mirasteilas Observatory in Falera. However, applying longer exposure times, these objects are also within the reach of average amateur equipment!

The processing of the profiles with Vspec software yields about the following dispersion values [ $\text{\AA}/\text{pixel}$ ]: DADOS 200  $\text{L mm}^{-1}$ : 2.55, DADOS 900  $\text{L mm}^{-1}$ : 0.65 and SQUES echelle: 0.18. Data of the Sony chip ICX285AL: 1.4 megapixel, 2/3” monochrome CCD, pixel size 6.45  $\mu\text{m} \times 6.45 \mu\text{m}$ .

## 2.3 Processing of the Spectra

The monochrome fits-images have been processed with the standard procedure of IRIS [6]. In most cases, about 2–5 spectral profiles have been stacked, to achieve a reasonable noise reduction. The generating and analyzing of the final profile was subsequently performed with Vspec [7]. For longer exposure times a dark frame was subtracted, if necessary also the separately recorded light pollution (by IRIS or fitswork). The processing of “flat fields” was omitted.

For profiles recorded by the echelle spectrograph SQUES, each order was processed and calibrated separately, analogously to the DADOS spectra. Further in rare cases with a significantly increased noise level (recording of very faint objects), the profile was sometimes smoothed, using filters such as “Spline” provided by the Vspec software. The goal of this process here was exclusively to improve the recognizability of the documented lines. A reduction of the telluric  $\text{H}_2\text{O}/\text{O}_2$  absorptions in the yellow/red range of the spectral profile was omitted. Correspondingly, the



documentation of lines of lower resolved profiles has been cautious and rather restrained.

## 2.4 Calibration of the Wavelength

Most of the spectra have been calibrated, based on rest wavelengths of known lines and not absolutely with the calibration lamp. This prevents the profile, as a result of possibly higher radial velocities, appearing to be shifted on the wavelength axis. The focus here is on the presentation of the spectral class and not on the documentation of the individual star. The calibration with the light source was restricted to higher resolved spectra of very late spectral classes, extraordinary stars and of course applied to extragalactic objects. Generally the applied unit for the wavelength is ångstrom [ $\text{\AA}$ ]. According to convention such values are indicated with the prefix  $\lambda$  [2]. For instance 5000  $\text{\AA}$  corresponds to  $\lambda 5000$ . The values are mostly taken from the Vspec database “lineident,” according to the catalog of lines in stellar objects, ILLSS Catalog (Coluzzi 1993–1999, VI/71A). As usual in the optical spectral domain, the wavelength  $\lambda$  is based on “standard air.”

## 2.5 Display of the Intensity Scale and Normalization of the Profiles

With minor exceptions in all spectra the pseudo-continuum was removed. The according process is outlined in [3]. The profiles have been rectified, divided by the course of their own continuum. Thus, the intensity of the spectral lines becomes visually comparable over the entire range. Otherwise in a raw profile of a pseudo-continuum strong lines at the blue or red end of the spectrum appear to be optically as too weak and vice versa, weak lines in the middle part as too high. But just this reasonable correction may confuse beginners, if they try to find spectral lines of their uncorrected pseudo-continuum in the according flat and rectified atlas profile. This effect is demonstrated in [3].

An absolute flux calibration of the intensity profile would be extremely time consuming and demanding and is not necessary for the purpose of this atlas. However, with minor exceptions, the intensity of the rectified profiles was normalized to unity, so the medium continuum level yields about  $I_c = 1$ . Hence, for space saving reasons, the displayed wavelength axis is normally shifted upwards, recognizable on the according level of the intensity axis ( $I > 0$ ). In some cases only the intensity value of the shifted wavelength axis is labeled (Figure 2.1). In case of montages, showing several

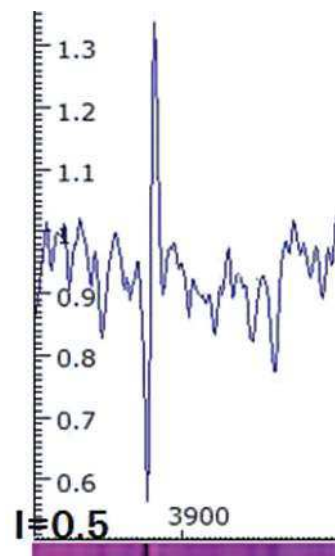


Figure 2.1 Labeling of the intensity scale, located here on the level  $I = 0.5$

spectra in one chart, the individual profiles have been normalized to unity, based on the same continuum section, to enable a rough comparison of the line intensities.

## 2.6 Identification and Labeling of the Spectral Lines

For line identification spectra commented on from the literature were used. In many cases, the sources are referenced accordingly. The aim was to specify two decimal places. If required some positions have been supplemented by the according Vspec databases, based on the ILLSS Catalog, Coluzzi 1993. In some cases NIST has also been consulted [8]. This way, a few intensive but undocumented lines have also been identified. However, this procedure was applied very restrictively, i.e. in few cases with a clear profile and a high line-intensity as well as missing plausible alternative elements in the immediate neighborhood. The labeling of such items is declared with a red “V.”

If appropriate in highly resolved SQUES echelle profiles, the lines are labeled with an accuracy of three decimal places – mostly based on SpectroWeb [9], or other referenced sources.

Blends of several spectral lines, appearing especially frequently in the mid to late stellar spectral classes, are usually labeled without decimal places. The most intense of the metal lines involved were mostly determined by SpectroWeb based on a comparable spectral class and in a few special cases even counter-checked by the *Bonner Spektralatlas* (BSA) [10].



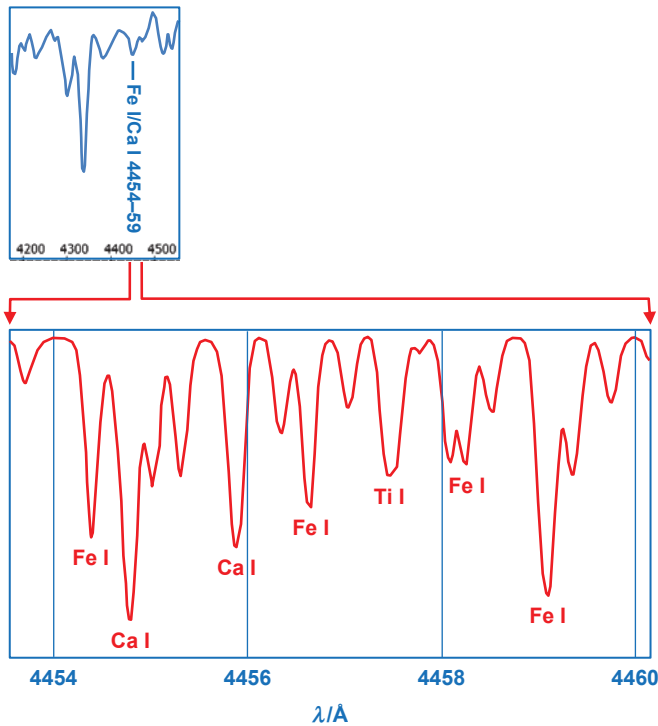



**Figure 2.2** Procyon,  $\alpha$  CMi, DADOS profile  $R \sim 900$  (above), compared to a corresponding resolution of  $R \sim 80,000$  (cut-out, schematically after SpectroWeb [9])

If the intensity of a blended line is clearly dominated by a certain element or ion, it is also used to label the whole blend.

Figure 2.2 shows using the example of Procyon how complexly composed even an inconspicuous small absorption can be, if displayed in a high-resolution profile. What in Plate 12 is roughly summarized as “Fe I/Ca I 4454–59,” turns out in SpectroWeb to be a highly complex blend of numerous metal lines.

## 2.7 Presentation

All spectra are at least documented by a broadband profile ( $200 \text{ L mm}^{-1}$ ). In the presence of interesting lines or according information, higher resolved spectra are attached, recorded with the  $900 \text{ L mm}^{-1}$  or in some special cases even with the SQUES echelle spectrograph. The line profiles are supplemented on the wavelength axis by synthetically generated 1D-spectra (by Vspec). Their color gradient is chiefly intended as a rough visual reference for the wavelength domain. Molecular absorption bands are marked with this icon, indicating the direction of fading intensity: .

## 2.8 Object Coordinates

With exception of the quasar list in Appendix H, this atlas contains no coordinates for the individual objects. Today the corresponding data for different epochs can easily be found online, either in the CDS [11] or NED database [12], and for brighter objects also in the numerous existing planetarium programs. Many such objects are further implemented even in the control software of today’s standard amateur telescopes and can be directly approached this way (Goto).

## 2.9 Distances

Distance information is given in light years [ly] or parsec [pc], where  $1 \text{ pc} \approx 3.26 \text{ ly}$ . For extragalactic objects often the  $z$ -value is applied, directly depending on the measured red- or blueshift in the spectrum (Section 26.10).